EFECTOS GRAVITATORIOS EN LA RETRACCIÓN DE FILAMENTOS LÍQUIDOS APOYADOS SOBRE UN PLANO INCLINADO

GRAVITY EFFECTS IN THE RETRACTION OF LIQUID FILAMENTS RESTING ON AN INCLINED PLANE

P. D. Ravazzoli*[1], A. G. González[1] y J. A. Diez[1]

[1] *Instituto de Física Arroyo Seco, Universidad Nacional del Centro de la Provincia de Buenos Aires, and CIFICEN-CONICET-CICPBA, Pinto 399, 7000, Tandil, Argentina.*

Recibido: 06/09/2021; Aceptado: 16/11/2021

En este trabajo estudiamos la retracción de filamentos líquidos apoyados sobre sustratos sólidos inclinados en condiciones de mojabilidad parcial. Debido a esto, cada extremo del filamento retrae longitudinalmente dando lugar a la formación de una región de acumulación de masa (cabeza) cerca del extremo, donde subsecuentemente se desarrolla un cuello en su parte posterior. Luego, este cuello se rompe formando una gota separada, mientras que el resto del filamento reinicia la secuencia de formación de cabeza con cuello y su posterior ruptura. En el caso horizontal, este proceso es simétrico y conduce a un arreglo regular de gotas equiespaciadas. Cuando el sustrato se encuentra inclinado, la gravedad actúa de manera diferente en cada extremo, modificando la distancia retraída por cada extremo hasta el momento de la ruptura, como así también la velocidad de retracción y la distancia final entre gotas la cual, además, deja de ser uniforme. Encontramos que, en el caso del plano inclinado, la distancia máxima que retrae el extremo que recede en contra (a favor) de la gravedad disminuye (aumenta) respecto del caso horizontal. Este efecto resulta ser un mecanismo útil para el auto–posicionamiento de las gotas resultantes al final del proceso. Nuestros resultados experimentales, tales como posiciones de los extremos, perfiles del espesor en el corte longitudinal, etc., son contrastados con simulaciones numéricas de las ecuaciones de Navier–Stokes, obteniéndose un buen acuerdo. Éste se ha logrado empleando como condición de contorno en la línea de contacto la relación de Cox–Voinov–Blake (CVB), la cual incluye tanto los efectos de la hidrodinámica macroscópica como así también de la dinámica molecular.

Palabras Claves: mojabilidad, filamentos, ángulo de contacto.

We study the retraction of liquid filaments resting on inclined solid substrates under partially wetting condition. This one causes each extreme of the filament to retract and form a region of mass accumulation (head) that subsequently develops a neck at its rear part. This neck then breaks up into a separate drop, while the rest of the filament restarts the sequence. In the horizontal case, this process is symmetric and leads to a regular arrangement of evenly spaced drops. When the substrate is inclined, gravity acts differently at each end, thus modifying the distance retracted by each end, the retraction speed and the final distance between drops, which also ceases to be uniform. We find that, in the case of the inclined plane, the maximum distance retracted by the end that recedes against (in favor of) gravity decreases (increases) with respect to the horizontal case. This effect turns out to be a useful mechanism for the self–positioning of the resulting drops at the end of the process. Our experimental results, such as end positions, thickness profiles in the longitudinal section, etc., are contrasted with numerical simulations of the Navier–Stokes equations, obtaining a good agreement. This is achieved by using in the contact line the boundary condition known as Cox–Voinov–Blake (CVB) relationship, which includes both the effects of macroscopic hydrodynamics as well as molecular dynamics.

Keywords: wettability, filaments, contact angle.

https://doi.org/10.31527/analesafa.2022.fluidos.52 ISSN 1850-1168 (online)

I. INTRODUCTION

In this work, we are concerned with the retraction and fragmentation of a long liquid filament sitting on an inclined substrate under partial wetting conditions. As schematically presented in Fig. 1(a), we focus our attention on the evolution of both extremes of the filament when the substrate inclination angle with respect to the horizontal is α. Once the liquid thread is placed on the incline, with its axis along the gravity component parallel to the plane, its ends start to *recede* along the longitudinal direction and *advance* in the transverse one. This process leads to the formation of a bulged region, here referred to as *head*. As a consequence of these combined motions a thinner region, called *neck*, is developed in the connecting region between the head and the rest of the filament that rapidly breaks up thus leading to a sessile drop that separates from the rest of the filament [1]. While the original head becomes a sessile drop, the rest of the filament repeats this process till a final arrangement of aligned drops is reached. A main feature of these drops is that the shape of their footprints is noncircular [2]. For the horizontal case, these drops are equally distanced [3], but this is not the case when the substrate is inclined (see Fig. 1(b)).

The physical mechanisms involved in the evolution of the head and its retraction in the horizontal case have been pre-

* pravazzoli@ifas.exa.unicen.edu.ar

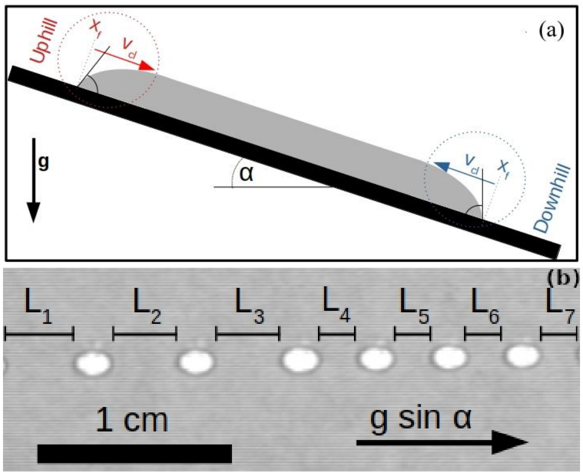

FIG. 1: (a) Scheme of the liquid filament placed on an inclined substrate with the axis of the filament along the gravity component parallel to the plane. (b) Final drop arrangement after the complete breakup of a filament of length $L = 3.36$ cm and width $w = 0.6$ mm on a substrate inclined $\alpha = 12.5^{\circ}$. The segments named as L_i ($i = 1,\ldots,7$) are the retraction distances travelled by the contact line to form the drop separated from the remaining filament: L_1, L_2 and L_3 (L_4, L_5, L_6 and L_7) correspond to the uphill (downhill) extreme.

viously reported [4]. Here, the main goal is to determine the effects of the component of gravity along the incline and parallel to the axis of the filament on its dynamic evolution and the final drops arrangement. We measure the evolution of the height profiles of the filament in the xz–plane (longitudinal direction) and from that information we are able to determine the contact angle at the filament tips, θ_x, and their velocities, v_{cl}. When the breakup processes have come to an end, we measure the distance between drops for both uphill and downhill extremes.

Our results are contrasted with numerical simulations, which solve the Navier–Stokes equations with appropriate boundary conditions at the contact line. To do so, we employ a combination between the hydrodynamic model proposed by Cox [5] and Voinov [6] (CV model) and a molecular–kinetics one from Blake [7]. This combined model was first proposed by Petrov [8, 9] and more recently adjusted to the liquid–solid combination used here [4] and named as CVB model.

II. EXPERIMENTAL RESULTS

We place a liquid filament on an inclined substrate with the axis of the filament along the gravity component parallel to the plane. The liquid partially wets the substrate (glass microscope slide) that was coated with a fluorinated solution (EGC-1700 of 3M). We focus our interest on the axial dewetting of the tips of the filament, which is made of a silicone oil (polydimethylsiloxane, PDMS), with density $\rho = 0.97$ g/cm^3, viscosity $\mu = 21.7$ Poise and surface tension $\gamma = 21.0$ dyn/cm. The filaments are generated from a controlled impact of the substrate against a vertical jet of PDMS, thus obtaining a liquid thread on the substrate with uniform width and parallel straight contact lines [4]. The whole system is placed on a base inclined $\alpha = 12.5^{\circ}$ and the experiments where perform at room temperature ($T \approx 20^{\circ}$C).

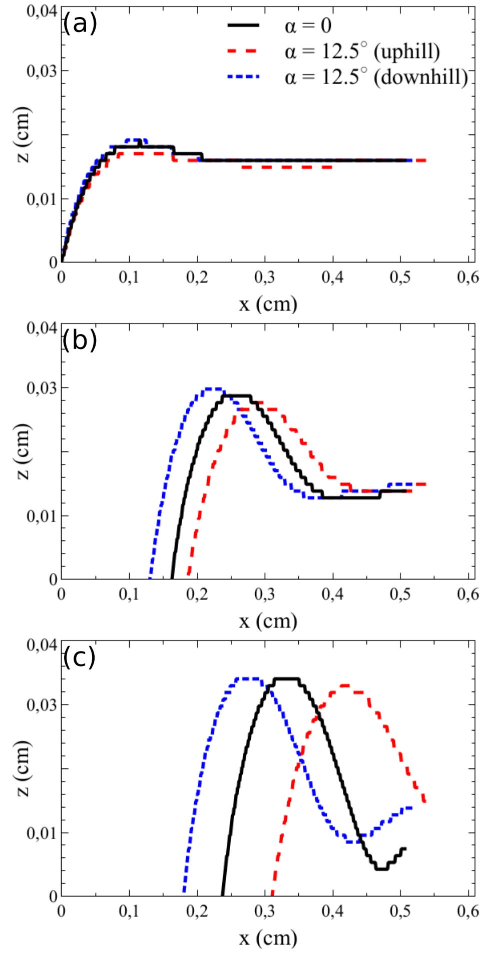

FIG. 2: Height profiles at the filament extremes for $\alpha = 0$ (both extremes are identical) and $\alpha = 12.5^{\circ}$ (uphill and downhill extremes) at different times: (a) $t = 0$ s, (b) $t = 50$ s and (c) $t = 100$ s.

The evolution of an inclined filament is similar to that of a horizontal one. While in that case, the dewetting and breakup mechanism repeats itself until a regular arrangement of drops is formed, in the inclined plane case, the retraction distances of the tips of the filament, x_f, are different because of gravity effects ($x_f(t) \geq 0$ for $t \geq 0$). Consequently, the space between the resulting drops also differs. It should be mentioned that the inclination angle, α, needs to be small enough so that the formed drops remain static and do not slide over the substrate leading to drop coalescence [10].

From the lateral observation of the filament evolution (side view) we are able to obtain the height profiles of the head region at any time. In Fig. 2 we show these profiles for both the horizontal and inclined cases at some selected times. We firstly observe that the downhill (uphill) tip recedes slower (faster) for $\alpha = 12.5^{\circ}$ than for $\alpha = 0$. From these profiles we measure the position of the tip, x_f, as a function of time, whose results are shown in Fig. 3. At early times ($t < 20$ s), the gravity effects are not yet important. For later times, the case with inclined plane shows that the downhill (uphill) tip recedes slower (faster) than the horizontal case. This implies that the maximum retraction distance (achieved when the receding processes stop) becomes smaller (larger) for the downhill (uphill) extreme.

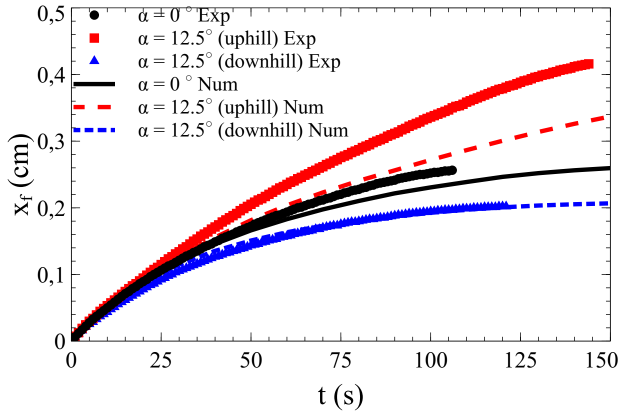

FIG. 3: Time evolution of the filament tips. The symbols correspond to the experimental data: black circles to $\alpha = 0$, while red squares and blue triangles to uphill and downhill tips, respectivley, for $\alpha = 12.5°$. The lines correspond to the results of the numerical simulation: black solid line to $\alpha = 0$, while red and blue dashed lines to uphill and downhill tips, respectively, for $\alpha = 12.5°$.

TABLE 1: Retraction lengths: Distances travelled by the filament tip up to neck breakup and separated drop formation.

$\alpha = 12.5°$	Uphill	L_1	0.412 cm
		L_2	0.398 cm
		L_3	0.405 cm
	Downhill	L_4	0.216 cm
		L_5	0.211 cm
		L_6	0.208 cm
		L_7	0.210 cm

After the complete evolution of the filament, a configuration of separated drops is reached (Fig. 1(b)), so that we measure the distance, L_i, between them. These results are presented in Table 1. As expected, the distances between drops at the uphill extreme are larger than the ones for the horizontal case ($\approx$ 0.295 cm), while they are shorter at the downhill extreme. For a given inclination angle, each extreme shows a typical separation distance, within the experimental error. Therefore, the variation of α can be used as a method to control the distance between final drops.

III. NUMERICAL SIMULATIONS

Wettability model

In order to perform the numerical simulations we need to use a suitable boundary condition to describe the contact line dynamics. As mentioned above, we use a combined model first proposed by Petrov [8], that includes both the hydrodynamic and molecular aspects of the local fluid–solid interaction (CVB model). The model yields the following relationship between the contact angle, θ, and the velocity of the contact line, v_{cl},

$$\theta^3 = \arccos^3\left[\cos\theta_0 - \frac{1}{\Gamma}\sinh^{-1}\left(\frac{v_{cl}}{v_0}\right)\right] + 9\frac{\mu v_{cl}}{\gamma}\ln\left(\frac{a_c}{\ell}\right), \quad (1)$$

where θ_0 is the microscopic equilibrium contact angle, $a_c = \sqrt{\gamma/(\rho g)}$ is the capilary length (macroscopic length scale), and g is gravity. The microscopic length scale, ℓ, the characteristic velocity, v_0 and the dimensionless parameter, Γ, are of molecular origin and depend on both the frequency of molecular displacements at equilibrium and the average distance between adsortion sites. These parameters were measured and reported elsewhere [4] for the PDMS and glass previously coated with the fluorinated solution EGC-1700, which is the same liquid–substrate configuration used here. Their values are:

$$\theta_0 = 50.57°, \quad v_0 = 6.212\times10^{-7} cm/s, \qquad \ell = 8.302\times10^{-4} a_c, \quad \Gamma = 95.455. \quad (2)$$

In Fig. 4 we compare the experimental results of the contact angle at the tip, θ_x, as function of the contact line velocity, v_{cl} with the CVB model. The dots represent the experimental results for $\alpha = 0$ and $\alpha = 12.5°$ (uphill and downhill tips), while the solid line corresponds to Eq. (1) with the parameters in Eq. (2). The experimental error in θ is $\Delta\theta = \pm1°$, and in v_{cl} it is $\Delta v_{cl} = \pm1.1\times10^{-3}$ cm/s. This agreement between experiments over an inclined substrate and the CVB model, confirms that the relationship in Eq. (1) effectively represents a local phenomenon, non affected by the presence of gravity.

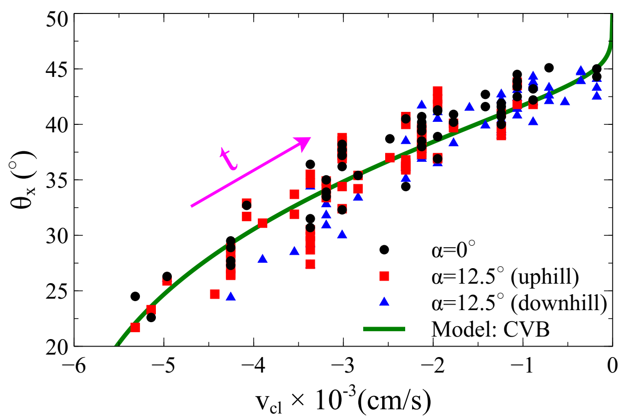

FIG. 4: Tip contact angle, θ_x, as function of the contact line velocity, v_{cl}. The symbols correspond to the experimental cases, $\alpha = 0$ (black) and $\alpha = 12.5°$ (red squares for uphill and blue triangles for downhill). The solid line shows the theoretical model (Eq. 1) and the arrow indicates the time evolution direction.

Time evolution

We obtain the time evolution of a liquid filament by numerically solving the dimensionless Navier–Stokes equation,

$$Re\left[\frac{\partial\vec{v}}{\partial t} + (\vec{v}\cdot\vec{\nabla})\vec{v}\right] = -\vec{\nabla}p + \nabla^2\vec{v} - \vec{z}\sin\alpha, \quad (3)$$

where $Re = \rho a_c \gamma/\mu^2$ is the Reynolds number. In our case, we have $Re = 0.14$, so that some slight inertial effects are considered in the simulations. Besides, we impose the boundary condition at the contact line as given by Eq. (1) by using the specific parameters for our liquid–solid configuration (see Eq. (2)). Since we have chosen a_c as the characteristic length of the problem, the corresponding Bond number is $Bo = \sin\alpha$.

The initial shape of the filament is represented by a cylin-

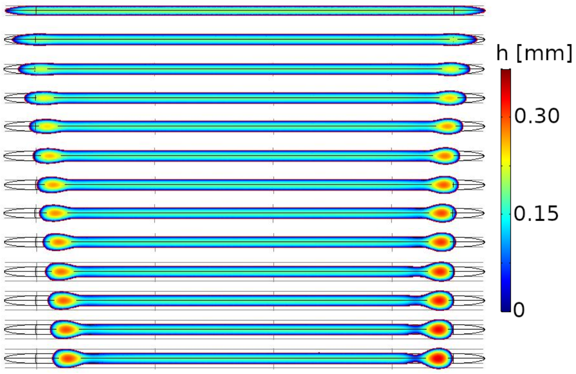

FIG. 5: Contour lines of the filament for $t = 0 - 130$ s every $\Delta t = 10$ s as given by the numerical simulation. At $t = 130$ s the downhill neck is formed and it is close to its breakup. At $t = 0$ the filament height is $h_0 = 0.02$ cm, its width is $w = 0.6$ cm, and its length is $L = 3$ cm.

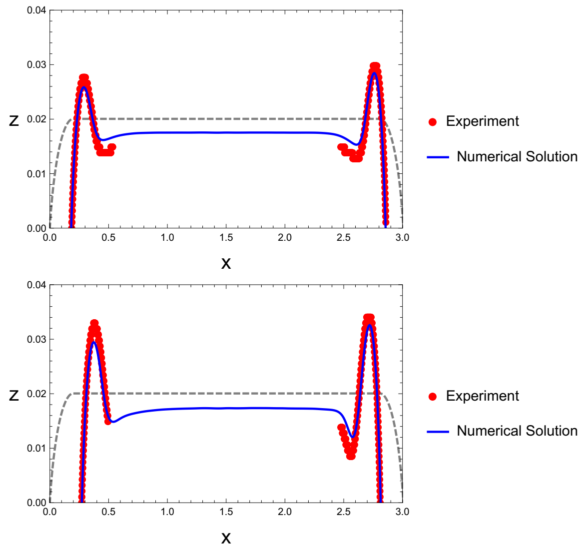

FIG. 6: Comparison between experimental and numerical height profiles. The gray dashed line corresponds to the initial numerical state, the solid blue line to the numerical solution and the red dots to the experimental profile. In order to compare the shape of the profile, the experimental data have been shifted so that the position of the tip is the same as in the numerical case. (a) $t = 50$ s and (b) $t = 100$ s.

drical cap with contact angle θ_0 along its sides. The extremes of the filament are shaped as halves of ellipsoidal caps with a contact angle at the tip, $\theta_x = 20°$. The ellipsoidal and cylindrical caps are matched with smooth continuity of thickness and contact angle.

Top views of the time evolution of the filament are shown in Fig. 5. As observed in the experiments, the simulations also yield that the downhill extreme recedes a shorter distance than the uphill one, till they break up and form the corresponding drops. Since the numerical method used here (moving mesh) does not allow for separations of the fluid into several domains, the code is unable to describe the complete breakup flow at the necks. Nevertheless, it is able to simulate the flow up to moments near the breakup, and its results remain useful for the purposes of the present work.

However, the retraction distances and the retraction velocities are smaller than those measured in the experiments. As shown in Fig. 3, the numerical simulation underestimates the displacement of the tip in the $\alpha = 0°$ case. This difference changes when the substrate is inclined. It becomes larger for the uphill extreme and smaller for the downhill one. In the latter case, the differences are practically negligible.

In Fig. 6 we compare the experimental and numerical height profiles for an inclined filament. In order to point out the shape differences, the experimental data have been shifted till the position of the experimental and numerical contact lines are coincident. It can be seen that for $t = 50$ s (Fig. 6(a)) the main differences are behind the heads of both extremes, in the neck regions, where the experimental profiles are a bit lower than the numerical ones. This departure is more pronounced for $t = 100$ s in the downhill neck, while the numerical head height is smaller than the experimental one at the uphill head. We believe that the differences at the uphill head and neck are related with the slower retraction of the tip as observed in Fig. 3.

IV. CONCLUSION

The experiments on the retraction of liquid filaments over an inclined substrate show that the presence of a longitudinal component of gravity produces an increase (decrease) of the retraction distance for the uphill (downhill) extreme necessary to produce each separated droplet. Moreover, as the breakup process repeats itself at each new filament extreme, we find that these retraction distances remain constant for all drops formed in both the uphill and downill portions of the initial filament (see Table 1).

It is interesting to point out that we confirmed the local behavior of the CVB wettability model. As we show in Fig. 4 the relationship $v_{cl}(\theta)$ measured for the uphill and downhill extremes of the filament is in good agreement with the model parametrized for the spreading of a circular drop over a horizontal substrate.

By using the CVB model in the simulations we found a good agreement with the experiments for early times respect to the breakup time (say $t < 30$ s, see Fig. 3). For $\alpha = 0$ and later times we observe that the simulation predicts lower retraction velocities of the extremes. This is due to the fact that the numerical method is unable to model complete breakups (or fluid domain separation), and thus it leaves a very thin filament connecting the almost separated drop from the remaining filament. The inclusion of a longitudinal volume force (gravity component parallel to the incline) for $\alpha > 0$ generates an additional downslope flow inside the filament such that it decreases (increases) the volume of the uphill (downhill) head due to the flow along the neck, which remains spuriously not broken for longer times due to the numerical flaw. This effect explains the even lower retraction velocity of the uphill extreme, and the compensation of this velocity at the downhill extreme, which is now increased respect to the $\alpha = 0$ case.

We consider that a complete understanding of the whole phenomenology still requires a more detailed physical model which, to our knowledge, is still unavailable in the literature. This type of flows constitute a simple method of technological interest to produce an arrange of self positioning drops with varying spacings.

REFERENCES

[1] A. G. González, J. Diez, R. Gratton y J. Gomba. Rupture of a fluid strip under partial wetting conditions. Europhys. Lett. **77,** 44001 (2007).

[2] P. D. Ravazzoli, A. G. González y J. A. Diez. Drops with non-circular footprints. Phys. Fluids **28,** 042104 (2016).

[3] I. Cuellar, P. D. Ravazzoli, J. A. Diez y A. G. González. Drop pattern resulting from the breakup of a bidimensional grid of liquid filaments. Physics of Fluids **29,** 102103 (2017).

[4] P. D. Ravazzoli, I. Cuellar, A. G. González y J. A. Diez. Wetting and dewetting processes in the axial retraction of liquid filaments. Phys. Rev. E **95,** 053111 (2017).

[5] O. V. Voinov. Hydrodynamics of wetting. Fluid Dyn. **11,** 714-721 (1976).

[6] R. G. Cox. The dynamics of the spreading of liquids on a solid surface. Part 1. Viscous flow. J. Fluid Mech. **168,** 169-194 (1986).

[7] T. D. Blake y J. M. Haynes. Kinetics of Liquid/Liquid Displacement. J. Colloid. Interface Sci. **30,** 421-423 (1969).

[8] P. G. Petrov y J. G. Petrov. A combined molecular–hydrodynamic approach to wetting kinetics. Langmuir **8,** 1762-1767 (1992).

[9] J. G. Petrov y R. V. Sedev. On the existence of a maximum speed of wetting. Colloids and Surfaces **13,** 313-322 (1985).

[10] P. D. Ravazzoli, I. Cuellar, A. G. González y J. A. Diez. Contact-angle-hysteresis effects on a drop sitting on an incline plane. Phys. Rev. E **99,** 043105 (2019).